

© 2018 Avinash N. Madavan

RISK-SENSITIVE SECURITY-CONSTRAINED ECONOMIC DISPATCH
VIA CRITICAL REGION EXPLORATION

BY

AVINASH N. MADAVAN

THESIS

Submitted in partial fulfillment of the requirements
for the degree of Master of Science in Electrical and Computer Engineering
in the Graduate College of the
University of Illinois at Urbana-Champaign, 2018

Urbana, Illinois

Adviser:

Assistant Professor Subhonmesh Bose

ABSTRACT

A security-constrained economic dispatch (SCED) problem is regularly solved by system operators in electric power networks to make day-ahead and real-time dispatch decisions. Preventive SCED is conservative and requires dispatch decisions that are secure against any single component failure. Corrective (recourse) actions can significantly reduce operational costs. Even with linear power flow models, corrective SCED poses significant computational challenges owing to an increase in the dimensionality arising from additional recourse decisions and the number of contingencies to guard against. This thesis analyzes the benefits of allowing recourse actions for simple networks and tackles the computational challenges of solving the problem at scale through a decomposition of the problem via a critical region exploration technique that exploits the problem structure using properties of multi-parametric linear programming. This thesis concludes with numerical results on various IEEE test networks.

*To my parents, brother, and grandfather
for their love and support.*

ACKNOWLEDGMENTS

I would like to thank my advisor, Professor Subhonmesh Bose, as well as Professor Lang Tong of Cornell University and Professor Ye Guo of Tsinghua-Berkeley Shenzhen Institute for their guidance in this research.

This work was partially supported by the International Institute of Carbon-Neutral Energy Research (I²CNER) and the Power System Engineering Research Center (PSERC).

TABLE OF CONTENTS

CHAPTER 1	INTRODUCTION	1
CHAPTER 2	EXISTING FORMULATIONS	4
2.1	The nominal ED problem	4
2.2	Existing security-constrained ED formulations	5
CHAPTER 3	THE RISK-SENSITIVE SECURITY-CONSTRAINED ECONOMIC DISPATCH (R-SCED) PROBLEM	8
3.1	A brief introduction to conditional value at risk	8
3.2	Risk-sensitive SCED	9
3.3	An illustrative 2-bus network example	11
CHAPTER 4	SOLUTION TECHNIQUE	15
4.1	Critical region exploration	16
CHAPTER 5	NUMERICAL RESULTS	20
5.1	IEEE 14-bus network results	20
5.2	IEEE 30-bus network results	22
CHAPTER 6	REFERENCES	25
APPENDIX A	DETERMINING THE CRITICAL REGION PA- RAMETERS	28
A.1	Critical region parameters under degeneracy	29

CHAPTER 1

INTRODUCTION

An economic dispatch (ED) problem seeks to minimize dispatch costs, subject to the engineering constraints of a power grid, e.g., capacity limits on power generation and transmission line power flows. The resulting dispatch, however, may not be feasible in the event that one or more components in the network fails. System operators often seek a dispatch that is robust to all *single* potential outages. This is referred to as the $N-1$ *security criterion* for an N -component power system. That is, they impose additional constraints on the dispatch to maintain reliable operation when the power system faces the failure of a single transmission line, transformer, or generator failures. This enhanced formulation of the ED problem with additional constraints is referred to as the *security-constrained economic dispatch* (SCED) problem. SCED problems are routinely solved in today's power system operation - in clearing day-ahead markets and in making real-time dispatch decisions. A SCED problem tries to balance between the system operator's two conflicting goals - minimize system costs and maintain reliability of power delivery under contingencies. This thesis provides an analytical comparison of the various formulations of SCED that have appeared in the literature over simple networks, extends the formulation in a way that better captures the tradeoff between cost and reliability, and finally prescribes an algorithm to deal with the computational difficulties of SCED with linearized power flow models.

SCED formulations abound in the literature, the first of which is *preventive*-SCED (P-SCED). This formulation imposes that the dispatch remain feasible within existing transmission line and generator capacity limits for all operational components in every contingency (cf. [1]). P-SCED does not consider potential recourse actions one can take when an outage occurs. The result is overly conservative and this formulation offers immediate extensions.

Notably, *corrective*-SCED (C-SCED) seeks to expand upon P-SCED by allowing active network components to respond to a contingency (cf. [2]).

It allows re-dispatch of generators with fast-ramping capabilities and some even allow partial load-shedding. A variety of formulations for C-SCED exist. More recent ones, e.g., in [3, 4, 5], have considered potential relaxation of transmission line limits immediately after a contingency occurs. Stricter limits are again enforced when recourse actions are taken. Section 3.3 offers a comparative analysis of the various SCED formulations on a simple 2-bus power network example, very much in line with the analysis in [6].

The authors in [3, 4, 5] seek to minimize the cost of nominal dispatch but ignore the costs associated with recourse actions. Recourse decisions – especially load shedding – can be costly when modeled via a *value of lost load*. To remedy that, the authors in [7] associate probabilities to contingencies and propose to minimize the expected dispatch costs across scenarios. The formulation is extended to one that aims to minimize the *conditional value at risk* (CVaR) of said costs. CVaR_α of a random variable measures the expected loss in the $\alpha\%$ -worst outcomes. As will be clear in the formulation in Chapter 3, the SO can express its preference in trading off cost versus reliability through its choice of α in our formulation.

Optimizing the recourse decision in each contingency requires the solution of an ED problem that is coupled to the nominal dispatch through ramping constraints of various generators. Regardless of formulation, the problem description of C-SCED is many times larger than a nominal ED problem. Scalably solving such problems on practical power networks then becomes challenging, especially for computing real-time dispatch decisions within strict time constraints. Two approaches have been advocated to deal with the attending computational difficulties. The first approach pre-filters contingencies; see [8, 9, 10, 11, 12, 13, 14] for a non-exhaustive list. In the second approach, one decomposes the C-SCED problem into multiple, significantly smaller optimization problems that can be solved in parallel and aggregated appropriately, e.g., see an accelerated augmented Lagrangian based method in [15] and using Bender’s decomposition in [16, 17, 18, 19, 20]. A decomposition based approach is adopted and a *critical region exploration* (CRE) algorithm for C-SCED and its risk-sensitive variant is presented in Section 4.1, that has recently been proposed for multi-area ED problems in [21]. With linear power flow models, C-SCED is a linear program, where the ED problem for deciding optimal recourse actions in each contingency becomes a linear program linearly parameterized by the nominal dispatch, where the

nominal dispatch refers to the dispatch under no contingencies. A method that systematically explores the space of nominal dispatch to arrive at the optimal solution is developed, leveraging properties of multi-parametric linear programming. The ED problems for the recourse decisions can be parallelized, leading to speed-ups compared to centralized solution techniques. The efficiency of this algorithm is numerically explored on various IEEE test networks in Chapter 5.

Part of this work has been submitted to IEEE PES General Meeting 2019 for possible presentation.

CHAPTER 2

EXISTING FORMULATIONS

In this section, the formulation for the nominal economic dispatch problem is presented. The notation for the nominal case is then used to develop the security-constrained counterparts.

2.1 The nominal ED problem

Consider an electrical power network on n buses, labeled $1, \dots, n$ with m transmission lines. Let each bus be equipped with a dispatchable generator and a nominal load. Let $\mathbf{g} \in \mathbb{R}^n$ and $\bar{\mathbf{d}} \in \mathbb{R}^n$ denote the vectors of nodal power generation and nominal demands, respectively. A linearized power flow model using DC approximations is assumed throughout.¹

The (directional) power flows over the transmission lines become linear maps of the vector of nodal power injections \mathbf{x} , given by $\mathbf{H}\mathbf{x}$. Here, $\mathbf{H} \in \mathbb{R}^{2m \times n}$ denotes the injection shift-factor matrix that depends on the topology of the power network and the admittances of the transmission lines. Denoting the limits on the (directed) power flows by $\mathbf{f} \in \mathbb{R}^{2m}$, the set of allowable nodal power injections can be represented as

$$\mathbb{P} := \{\mathbf{x} \in \mathbb{R}^n \mid \mathbf{H}\mathbf{x} \leq \mathbf{f}, \mathbf{1}^\top \mathbf{x} = 0\}, \quad (2.1)$$

where $\mathbf{1} \in \mathbb{R}^n$ is a vector of all ones. The equality constraint, $\mathbf{1}^\top \mathbf{x} = 0$, captures the balance of demand and supply of power across the network. The DC approximations deem the voltage magnitudes to be at their nominal values, ignore transmission line losses, and assume voltage phase angle differences across neighboring buses to be small. One can utilize real-time measurements to estimate \mathbf{H} , e.g., in [22].

¹All formulations can easily be extended to any linear power flow model.

Assume a linear cost of production $\mathbf{c}^\top \mathbf{g}$ for producing \mathbf{g} from dispatchable generators that can vary their outputs within $\mathbb{G} = [\underline{\mathbf{G}}, \overline{\mathbf{G}}]$. The lack of a generator at a bus i can be modeled by letting $\underline{G}_i = \overline{G}_i = 0$. With the above notation, the nominal ED problem is given by

$$\begin{aligned} & \underset{\mathbf{g}}{\text{minimize}} && \mathbf{c}^\top \mathbf{g}, \\ & \text{subject to} && \mathbf{g} \in \mathbb{G}, \mathbf{g} - \bar{\mathbf{d}} \in \mathbb{P}. \end{aligned} \tag{2.2}$$

2.2 Existing security-constrained ED formulations

Problem (2.2) minimizes system operational costs subject to network constraints. However, the generation profile does not guard against possible component failures. To define a security-constrained variant, consider a collection of scenarios, denoted $1, \dots, K$, each of which corresponds to a single transmission line failure. A line outage alters the network topology and manifests in the ED problem as a different injection shift factor matrix \mathbf{H}^k . The formulation of the security-constrained variant depends on possible recourse actions one can take in each contingency. The following section presents different formulations of security-constrained economic dispatch (SCED) problems and discusses their pros and cons.

2.2.1 Preventive-SCED

Perhaps the most conservative of approaches, preventive SCED, stipulates that \mathbf{g} must be able to satisfy the nominal demands even after any single line failure, and hence, it solves the following P-SCED problem:

$$\begin{aligned} & \underset{\mathbf{g}}{\text{minimize}} && \mathbf{c}^\top \mathbf{g}, \\ & \text{subject to} && \mathbf{g} \in \mathbb{G}, \mathbf{g} - \bar{\mathbf{d}} \in \mathbb{P}, \mathbf{g} - \bar{\mathbf{d}} \in \mathbb{P}^k, \\ & && k = 1, \dots, K. \end{aligned} \tag{2.3}$$

Here, \mathbb{P}^k is the feasible injection region in the k -th contingency, that is identical to (2.1), except that \mathbf{H} is replaced by \mathbf{H}^k . It effectively shrinks the set of generation profiles, resulting in higher generation costs. See [6] for an analysis of the additional costs for simple network topologies.

2.2.2 Corrective-SCED

The corrective counterpart allows for recourse decisions, and is therefore able to provide security against outages at a possibly lower operational cost than P-SCED. Various formulations of the corrective variant C-SCED are known; the following description mirrors that in [5]:

$$\begin{aligned}
& \text{minimize} && \mathbf{c}^\top \mathbf{g}, \\
& \text{subject to} && \mathbf{g} \in \mathbb{G}, \mathbf{g} - \bar{\mathbf{d}} \in \mathbb{P}, \mathbf{g} - \bar{\mathbf{d}} \in \mathbb{P}_{\text{DA}}^k, \\
& && \mathbf{g} + \delta \mathbf{g}^k \in \mathbb{G}, \mathbf{g} + \delta \mathbf{g}^k - \bar{\mathbf{d}} \in \mathbb{P}_{\text{SE}}^k, |\delta \mathbf{g}^k| \leq \Delta_{\mathbf{g}}, \\
& && \text{for } k = 1, \dots, K
\end{aligned} \tag{2.4}$$

over $\mathbf{g}, \delta \mathbf{g}^1, \dots, \delta \mathbf{g}^K$. The deviation of the supply from the generators in contingency k from the nominal case is denoted by $\delta \mathbf{g}^k$. Here, $\Delta_{\mathbf{g}}$ models the ramping constraints. The inequality $|\delta \mathbf{g}^k| \leq \Delta_{\mathbf{g}}$ is interpreted elementwise, i.e., $|\delta \mathbf{g}_i^k| \leq \Delta_{\mathbf{g},i}$.

Apart from allowing recourse decisions, notice that (2.4) allows post-contingency but pre-recourse nodal power injections to take values in \mathbb{P}_{DA}^k , and those during the recourse action to take values in \mathbb{P}_{SE}^k , where

$$\mathbb{P}^k \subset \mathbb{P}_{\text{SE}}^k \subset \mathbb{P}_{\text{DA}}^k.$$

Subscript DA and SE stand for *drastic action* and *short-term emergency* limits, respectively. Sets $\mathbb{P}_{\text{DA}}^k, \mathbb{P}_{\text{SE}}^k$ are essentially identical to \mathbb{P}^k with larger line capacity limits. These capacities are primarily defined by thermal considerations of transmission lines and transformers. Such components can usually withstand power flows higher than their rated values for short time periods – drastic action limits for about 5 minutes and short-term emergency limits for about 15 minutes. Figure 2.1 provides an illustration of these limits with the addition of the *long-term emergency* (LE) limit. These dynamic ratings ensure that the line does not exceed its maximum thermal capacity over the operating interval. For a better description of the limits used in practice see [23].

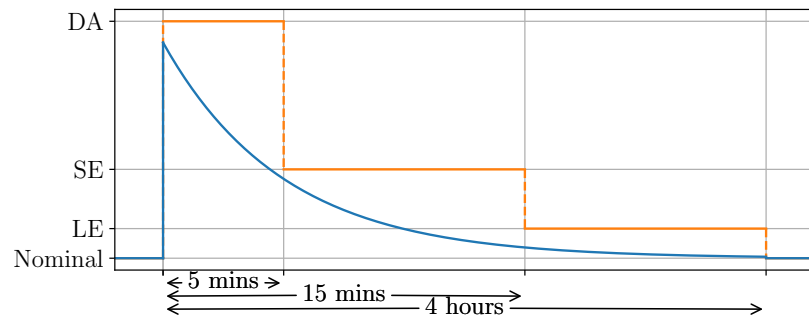


Figure 2.1: An example of (—) dynamic lines ratings based on [23] with (—) one possible realization of line flows.

CHAPTER 3

THE RISK-SENSITIVE SECURITY-CONSTRAINED ECONOMIC DISPATCH (R-SCED) PROBLEM

To gain a more nuanced handle on the tradeoff between procurement costs and reliability of power delivery, now expand the formulation of C-SCED (2.4). Allow load shedding and consider a risk-sensitive objective function that accounts for recourse costs. The proposed formulation utilizes the *conditional value at risk* (CVaR) in defining the objective function of the R-SCED problem. Section 3.1 briefly explains this risk measure before the formulation of R-SCED is presented in Section 3.2.

3.1 A brief introduction to conditional value at risk

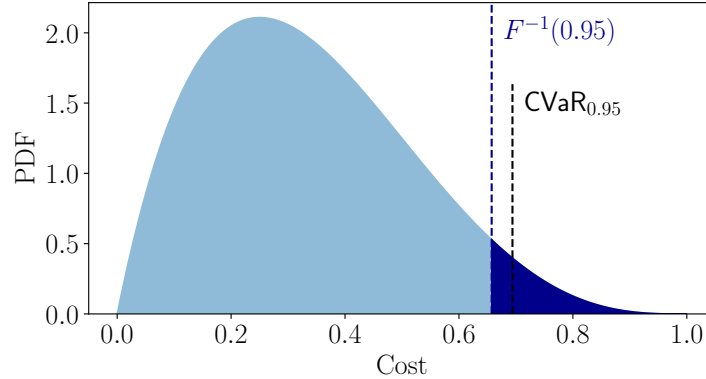


Figure 3.1: The probability density function of some cost where the shaded region denotes the tail of the distribution occurring with probability 0.05.

The *conditional value at risk* (CVaR) is a risk measure that maps a random cost to a scalar value. This risk measure provides a parameter α that captures one's willingness to accept high losses for the sake of profit. To express this formally, consider a random cost, χ . The $\text{CVaR}_\alpha[\chi]$ denotes the expected

cost of the $(1 - \alpha)$ fraction of highest cost outcomes, or

$$\text{CVaR}_\alpha[\chi] := \mathbb{E}[\chi | \chi \geq F^{-1}(1 - \alpha)],$$

where F is the cumulative distribution function of χ and \mathbb{E} denotes the expected value over that distribution. Figure 3.1 provides an example for some probability distribution of the random cost, χ . The shaded region denotes the tail of the distribution occurring with probability 0.05, and $\text{CVaR}_{0.95}[\chi]$ computes the expected value over this tail distribution. Observe that CVaR computes the expected value of χ when $\alpha = 0$. As α increases, only higher and higher cost scenarios are considered, so that if α increases to 1 only the highest cost scenario is considered.

Optimization using CVaR first found appeal in financial literature for portfolio risk-mitigation [24]. More recently, it has been proposed for a number of power systems applications. In [25], the author proposes using a CVaR objective to determine self-scheduling for power producers under price uncertainty. Several papers use CVaR -based constraints to ensure lines remain within ratings under uncertainty due to renewable generation [26, 27, 28].

The risk-sensitive SCED problem formulation in Section 3.2 penalizes the conditional value at risk of the dispatch costs across all contingencies. Cost in any contingency depends on two factors – the dispatch decisions and the realized contingency. For a given dispatch, the cost is a random variable defined over the set of possible contingencies. The expectation and CVaR of this random variable can easily be computed. Optimizing over the CVaR of the dispatch cost is equivalent to determining the dispatch decisions for which the CVaR of cost is minimized. The result is the dispatch for which the cost in the $(1 - \alpha)$ fraction of the most expensive contingencies is the lowest.

3.2 Risk-sensitive SCED

Let the satisfied nodal demand be allowed to vary between a minimum load level $\underline{\mathbf{d}}$ and the nominal $\bar{\mathbf{d}}$. Denote the amount of load shed as $\delta \mathbf{d}^k \in [0, \bar{\mathbf{d}} - \underline{\mathbf{d}}] := \Delta_d$. Associate probabilities $\mathbf{p} \in \mathbb{R}^K$ to the contingencies, where $p_0 := 1 - \mathbf{1}^\top \mathbf{p}$ represents the probability of the nominal state. Define the *risk-*

sensitive SCED (R-SCED) problem as

$$\text{minimize } \text{CVaR}_\alpha [\mathbf{c}^\top \mathbf{g} + C(\delta \mathbf{g}, \delta \mathbf{d})], \quad (3.1a)$$

$$\text{subject to } \mathbf{g} \in \mathbb{G}, \mathbf{g} - \bar{\mathbf{d}} \in \mathbb{P}, \quad (3.1b)$$

$$\mathbf{g} - \bar{\mathbf{d}} \in \mathbb{P}_{\text{DA}}^k, \quad (3.1c)$$

$$\mathbf{g} + \delta \mathbf{g}^k \in \mathbb{G}, \quad (3.1d)$$

$$\mathbf{g} + \delta \mathbf{g}^k - \bar{\mathbf{d}} + \delta \mathbf{d}^k \in \mathbb{P}_{\text{SE}}^k, \quad (3.1e)$$

$$|\delta \mathbf{g}^k| \leq \Delta_g, \delta \mathbf{d}^k \in \Delta_d, \quad (3.1f)$$

for each $k = 1, \dots, K$,

over \mathbf{g} , $\delta \mathbf{g}$, $\delta \mathbf{d}$. Here, $\delta \mathbf{g}$, $\delta \mathbf{d}$ denote the collection of the respective variables across all contingencies. Additionally, $C(\delta \mathbf{g}, \delta \mathbf{d})$ is the recourse cost, assuming a contingency occurs. It is a random variable and takes the value

$$C^k(\delta \mathbf{g}^k, \delta \mathbf{d}^k) := \mathbf{c}^\top \delta \mathbf{g}^k + \mathbf{v}^\top \delta \mathbf{d}^k$$

in contingency k . Here, \mathbf{v} measures the vector of nodal values of lost load (VoLL).¹ The formulation in (3.1) generalizes that in [7] that seeks to minimize expected recourse costs. Instead, (3.1) minimizes its CVaR, the conditional value at risk.

Notice that the values of lost load are usually higher than generation costs [29]. Therefore, the larger the α (or α'), the less the system operator is inclined to shed load and thereby prioritize reliability. As a result, RSCED provides the operator a better handle to explore the tradeoff between dispatch cost and reliability of power delivery.

Next, consider a property of RSCED, the proof of which proves useful in devising an algorithm to solve it in Section 4.1.

Proposition 1. *The optimal cost of (3.1) is piecewise affine in α' over any interval in \mathbb{R}_+ . Additionally, the optimal nominal dispatch \mathbf{g}^* remains constant over sub-intervals where the optimal cost is affine.*

Proof. Observe that $\mathbf{c}^\top \mathbf{g} + C(\delta \mathbf{g}, \delta \mathbf{d})$ takes values in a discrete set with probabilities \mathbf{p} . Letting $C^0 = 0$ and $p^0 = 1 - \mathbf{1}^\top \mathbf{p}$ for the nominal case, the

¹The cost structure can be altered to distinguish between different costs for regulation up and down, i.e., by replacing $\mathbf{c}^\top \delta \mathbf{g}^k$ in the recourse cost by $\mathbf{c}_+^\top [\delta \mathbf{g}^k]^+ + \mathbf{c}_-^\top [-\delta \mathbf{g}^k]^+$ without adding conceptual difficulties.

objective function of (3.1) using (3.1) becomes

$$\min_z \left\{ z + \alpha' \sum_{k=0}^K p^k \left[\mathbf{c}^T \mathbf{g} + C^k(\delta \mathbf{g}^k, \delta \mathbf{d}^k) - z \right]^+ \right\}. \quad (3.2)$$

Using the epigraph form, (3.1) then reduces to solving

$$\begin{aligned} & \underset{z, \mathbf{y}, \mathbf{g}, \delta \mathbf{g}, \delta \mathbf{d}}{\text{minimize}} && z + \alpha' \sum_{k=0}^K p^k y^k, \\ & \text{subject to} && y^k \geq 0, \\ & && y^k \geq \mathbf{c}^T \mathbf{g} + C^k(\delta \mathbf{g}^k, \delta \mathbf{d}^k) - z, \\ & && (3.1b) - (3.1f), \\ & && \text{for each } k = 1, \dots, K, \end{aligned} \quad (3.3)$$

where $\mathbf{y} := (y_0, \dots, y_K)^\top$. More compactly, define

$$\mathbf{x}^0 := (z, y^0, \mathbf{g}^\top)^\top, \quad \mathbf{x}^k := (y^k, [\delta \mathbf{g}^k]^\top, [\delta \mathbf{d}^k]^\top)^\top,$$

and rewrite (3.3) as

$$\begin{aligned} & \underset{\mathbf{x}^0, \mathbf{x}^1, \dots, \mathbf{x}^K}{\text{minimize}} && [\mathbf{c}^0]^\top \mathbf{x}^0 + \alpha' \sum_{k=1}^K [\mathbf{c}^k]^\top \mathbf{x}^k, \\ & \text{subject to} && \mathbf{A} \mathbf{x}^0 \leq \mathbf{b}, \\ & && \mathbf{A}^k \mathbf{x}^0 + \mathbf{E}^k \mathbf{x}^k \leq \mathbf{b}^k, \\ & && k = 1, \dots, K, \end{aligned}$$

for suitably defined $\mathbf{A}, \mathbf{b}, \mathbf{A}^k, \mathbf{E}^k, \mathbf{b}^k, \mathbf{c}^0, \mathbf{c}^k$. This is a parametric linear program linearly parameterized by α' . The proof then follows from [30, Theorem 7.2]. \square

3.3 An illustrative 2-bus network example

This section considers a simple 2-bus network. The solutions of the R-SCED problem are computed and compared with the solutions of the P-SCED and C-SCED formulations.

Table 3.1: Comparison of nominal dispatch and its cost under various ED formulations.

Method	g_1^* (MW/hr)	g_2^* (MW/hr)	Nominal Cost (\$/hr)
ED	20.0	0.0	20.0
P-SCED	15.0	5.0	25.0
C-SCED	17.25	2.75	22.75
C-SCED _{aug}	18.75	1.25	21.75
R-SCED (0.1)	18.75	1.25	21.25
R-SCED (0.9)	17.25	2.75	22.75

Recall that C-SCED (2.4) adds flexibility to P-SCED (2.3) in two ways – it relaxes the line capacity constraints immediately after a contingency occurs and allows generators to alter their outputs within a short period of time. We now analyze the impact of these flexibilities on the cost of nominal dispatch for a two-bus network example shown in Figure 3.2.

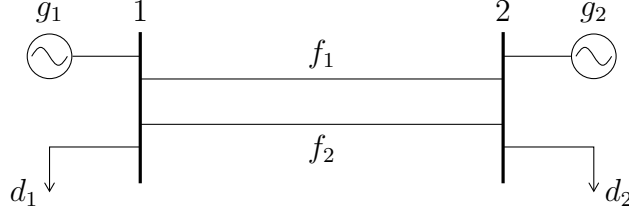


Figure 3.2: A two-bus network example.

Now consider the solution of ED, P-SCED, C-SCED, and R-SCED on the 2-bus network example in Figure 3.2. Consider the parameter values $c_1 = \$1/\text{MW}$, $c_2 = \$2/\text{MW}$. Thus, generator at bus 1 is cheaper than that at bus 2. Let $\Delta_{g_1} = 0.25 \text{ MW/min}$, $\Delta_{g_2} = 0.2 \text{ MW/min}$, i.e., the cheaper generator is more flexible. Let both buses have identical demands of 10 MW, and assume uniform value of lost load of $\$30/\text{MW}$ at both buses. The transmission line capacities are given by $f_1 = 5 \text{ MW}$ and $f_2 = 7 \text{ MW}$. Assume identical probability of line failures, given by $p_1 = p_2 = 0.01$. Finally, let $\mathbf{f}_{DA} = 1.75\mathbf{f}$ and $\mathbf{f}_{SE} = 1.25\mathbf{f}$. Table 3.1 captures the nominal dispatch cost under various formulations of ED on the 2-bus example.

Consider a special case of C-SCED denoted by C-SCED_{aug} that is augmented to allow for potential load shed and minimizes the expected cost

of generation including the costs associated with regulation and load shed through the value of lost load. This mimics the formulation provided in this text except that the objective is in expectation and not CVaR.

Observe the R-SCED solution for low α recovers the C-SCED solution minimizing expected cost with load shed. Additionally, as α increases to 1, the R-SCED solution reduces to the C-SCED case without load shed. Note that for general power networks, the R-SCED solution is not equal to the C-SCED without load shed. The R-SCED formulation for high α weighs regulation as well as load shed more heavily than nominal generation resulting in different results.

Following Proposition 1, Figure 3.3 shows nominal dispatch cost and total load shed are piecewise constant. Also, as α increases, the nominal dispatch cost increases and the quantity of load shed decreases, thereby demonstrating α as a tunable parameter to trade-off between cost and network reliability.

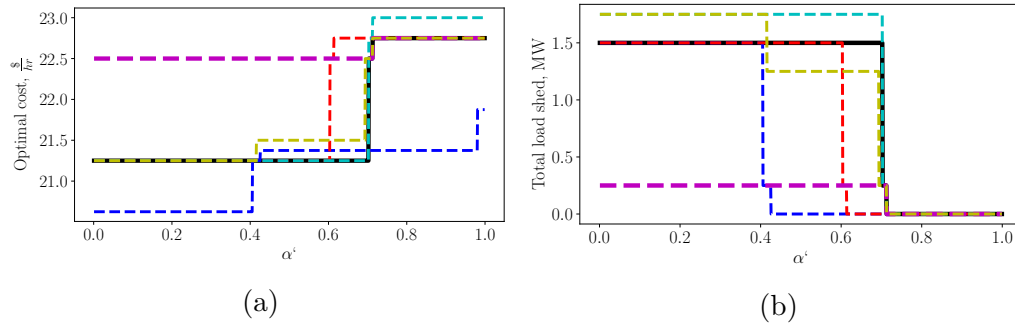


Figure 3.3: The effect of α on (a) nominal dispatch cost and (b) total load shed. Each plot denotes the 2-bus example augmented with (—) no augmentations, (---) dispatch cost at bus 2 reduced to $c_2 = 1.5$, (---) VoLL increased to $v = 40\$/\text{MW}$, (---) generation ramp limits reduced to $\Delta_{g_1} = 0.2 \text{ MW}$ and $\Delta_{g_2} = 0.15 \text{ MW}$, (-.-) drastic action limit set to $f_{\text{DA}} = 1.5f$, and (-.-.-) reduced higher capacity line limit $f_2 = 6 \text{ MW}$.

The R-SCED problem balances recourse cost associated with both regulation and load shed with nominal cost of generation. The importance of this distinction is illustrated in the case when cost of expensive generation decreases and, by extension, the cost of the associated regulation decreases. Notice, in this example, the cost of nominal generation exceeds that of the nominal case briefly and the cost of nominal generation increases for high α despite no change in load shed. The former results from the relatively higher value of lost load, which reduces earlier. The latter is the result of R-SCED

balancing the cost associated with regulation with the nominal cost. R-SCED prioritized its decrease over reducing regulation because of the higher associated cost, but the effect of regulation still remains.

CHAPTER 4

SOLUTION TECHNIQUE

From Proposition 1, R-SCED can be reformulated as a linear program (LP). A similar procedure can be used to reformulate C-SCED as an LP, however the precise details are omitted for brevity. Either linear program is challenging to solve due to its large size for practical power systems. To illustrate, consider for example the Polish power system with 2383 buses, 2869 lines, 327 generators, and 1817 loads. The nominal ED problem is over 327 variables and 6447 linear constraints. By comparison, the C-SCED can be formulated over 947319 variables and 28949071 linear constraints, while R-SCED requires an even greater 6212249 variables and 28954865 linear constraints. According to [20], the resulting linear program, due to its size, is not solvable by traditional LP methods. This is especially true for power systems requiring a solution in real-time. This section describes a method for decomposing the LP into smaller problems that are more computationally tractable and can easily be parallelized for greater speed, and a method for solving these decomposed problems is described in Section 4.1.

Recall, the R-SCED problem was previously shown to take the form

$$\begin{aligned}
 & \underset{\mathbf{x}^0, \mathbf{x}^1, \dots, \mathbf{x}^K}{\text{minimize}} && [\mathbf{c}^0]^\top \mathbf{x}^0 + \alpha' \sum_{k=1}^K [\mathbf{c}^k]^\top \mathbf{x}^k, \\
 & \text{subject to} && \mathbf{A}\mathbf{x}^0 \leq \mathbf{b}, \\
 & && \mathbf{A}^k \mathbf{x}^0 + \mathbf{E}^k \mathbf{x}^k \leq \mathbf{b}^k, \\
 & && k = 1, \dots, K.
 \end{aligned} \tag{4.1}$$

Observe that $\mathbf{x}^1, \dots, \mathbf{x}^K$ are independent of one another, both in the objective and constraints. One can exploit this property by decomposing the problem in a way that a master problem interacts with the following subproblems

that can be solved in parallel.

$$\begin{aligned} & \underset{\mathbf{x}^0}{\text{minimize}} && [\mathbf{c}^0]^\top \mathbf{x}^0 + \alpha' \sum_{k=1}^K J_k^*(\mathbf{x}^0), \\ & \text{subject to} && \mathbf{A}\mathbf{x}^0 \leq \mathbf{b}, \end{aligned} \tag{4.2}$$

where

$$\begin{aligned} J_k^*(\mathbf{x}^0) := & \underset{\mathbf{x}^k}{\text{minimize}} && [\mathbf{c}^k]^\top \mathbf{x}^k, \\ & \text{subject to} && \mathbf{A}^k \mathbf{x}^0 + \mathbf{E}^k \mathbf{x}^k \leq \mathbf{b}^k. \end{aligned} \tag{4.3}$$

The following section presents the *critical region exploration* (CRE) algorithms for solving these decomposed linear programs.

4.1 Critical region exploration

The CRE algorithm expounded in [21] adopts a technique exploiting the properties of multi-parametric linear programming. Properties of J_*^k are crucial to describe our algorithm. Additional notation is needed to describe them. Define

$$\mathbb{X}^0 := \{\mathbf{x} \mid \mathbf{A}\mathbf{x} \leq \mathbf{b}\}.$$

Assume throughout that (4.3) is feasible for any $\mathbf{x}^0 \in \mathbb{X}^0$. A collection of polyhedral sets $\mathbb{S}_1, \dots, \mathbb{S}_L$ define a *polyhedral partition* of \mathbb{S} , if all of the L sets are polyhedral, their union spans \mathbb{S} , and they only intersect possibly at their boundaries. One such example is provided in Figure 4.1. Given this definition, a vital property of J_*^k is recorded in the following lemma.

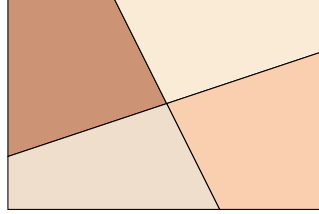


Figure 4.1: A graphical illustration of the intersection of critical regions induced by each sub-problem (4.3) for $k = 1, \dots, K$.

Lemma 1. $J_*^k(\mathbf{x}^0)$ is piecewise affine over \mathbb{X}^0 and the sets over which it is affine describe a polyhedral partition of \mathbb{X}^0 .

Problem (4.3) is a multiparametric linear program, linearly parameterized by \mathbf{x}^0 . As a consequence, its proof follows directly from [30, Theorem 7.2]. Hereafter, the sets in the polyhedral partition are called *critical regions*. For a given $\mathbf{x}^0 \in \mathbb{X}^0$, one can compute the critical region \mathbb{C}^k that contains $\mathbf{x}^0 \in \mathbb{X}^0$ and the affine description of the optimal cost J_*^k over \mathbb{C}^k for each $k = 1, \dots, K$. More precisely, let the affine description of J_*^k be given by $[\boldsymbol{\rho}^k]^\top \mathbf{x}^0 + \eta^k$ over \mathbb{C}^k . The procedure for determining this critical region and the associated affine cost description is relegated to Appendix A to maintain continuity of presentation. With the affine descriptions of J_*^1, \dots, J_*^K , solve

$$\begin{aligned} \underset{\mathbf{x}^0}{\text{minimize}} \quad & [\mathbf{c}^0]^\top \mathbf{x}^0 + \alpha' \left[\sum_{k=1}^K [\boldsymbol{\rho}^k]^\top \mathbf{x}^0 + \eta^k \right], \\ \text{subject to} \quad & \mathbf{A}\mathbf{x}^0 \leq \mathbf{b}, \\ & \mathbf{x}^0 \in \cap_{k=1}^K \mathbb{C}_k^0, \end{aligned} \tag{4.4}$$

i.e., (4.2) with the additional constraint $\mathbf{x}^0 \in \cap_{k=1}^K \mathbb{C}_k^0$, over which the affine description of J_*^k holds. The above problem can be solved as an LP. Assume that one can determine the *lexicographically smallest* minimizer of (4.4). This provides a tie-breaking technique in the case the minimizer is not unique. The final consideration is a necessary and sufficient condition for $[\mathbf{x}^0]^*$ to be the minimizer of (4.2). To that end, $[\mathbf{x}^0]^*$ is a minimizer for (4.2) if and only if

$$0 \in \delta J^*([\mathbf{x}^0]^*) + N_{\mathbb{X}^0}([\mathbf{x}^0]^*), \tag{4.5}$$

where $\delta J^*(\cdot)$ denotes the subdifferential set of the objective function of (4.2) and $N_{\mathbb{X}^0}$ the normal cone of \mathbb{X}^0 . With the notation at hand, Algorithm 1 to solve (4.1) can now be presented.

The following result sums up the crucial property of our algorithm.

Proposition 2. *Algorithm 1 converges to an optimizer of (4.1) in finitely many iterations.*

The proof is largely similar to that of [21, Theorem 1], and is omitted for brevity. For that proof technique to work, it is crucial that all variables in (4.2) and (4.3) remain bounded. Recall that (3.1) was reformulated as (3.3) and eventually as (4.1). Variable z in (3.3) in general is not bounded. The definition of CVaR allows us to bound z by the minimum and the maximum

Algorithm 1 Solving the risk-sensitive security-constrained optimal power flow problem

```

1: Initialize:
    $\mathbf{x}^0 \in \mathbb{X}^0, J^* \leftarrow \infty, \mathbb{D} \leftarrow \text{empty set}, \epsilon \leftarrow$ 
   small positive number
2: do
3:   Given  $\mathbf{x}^0$ , compute  $\boldsymbol{\rho}^k, \eta^k, \mathbb{C}^k$  for  $k = 1, \dots, K$ .
4:   Solve (4.4).
5:    $[\mathbf{x}^0]^{\text{opt}} \leftarrow$  lexicographically smallest minimizer of step 4.
6:    $J^{\text{opt}} \leftarrow$  optimal cost of step 4.
7:   if  $J^{\text{opt}} < J^*$  then
8:      $[\mathbf{x}^0]^* \leftarrow [\mathbf{x}^0]^{\text{opt}}, J^* \leftarrow J^{\text{opt}}, \mathbb{D} \leftarrow \{\mathbf{c}\}$ .
9:   else
10:     $\mathbb{D} \leftarrow \mathbb{D} \cup \{\mathbf{c}^0 + \alpha' \sum_{k=1}^K \boldsymbol{\rho}^k\}$ .
11:   end if
12:    $\mathbf{v}^* \leftarrow \operatorname{argmin}_{\mathbf{v} \in \operatorname{conv}(\mathbb{D}) + N_{\mathbb{X}^0}([\mathbf{x}^0]^*)} \|\mathbf{v}\|^2$ 
13:    $\mathbf{x}^0 \leftarrow [\mathbf{x}^0]^{\text{opt}} - \epsilon \mathbf{v}^*$ 
14: while  $v^* \neq 0$ 

```

value of C across contingencies. Since these costs are defined over compact sets, they remain bounded, and therefore, one can restrict z to an interval without affecting the optimal solution of (3.3).

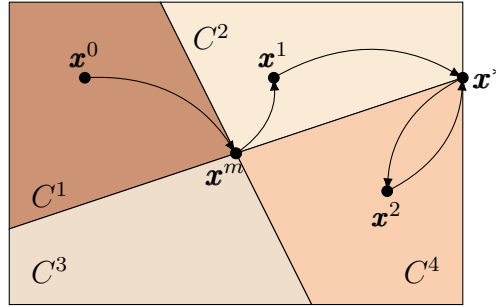


Figure 4.2: A graphical illustration of the intersection of critical regions induced by each sub-problem (4.3) for $k = 1, \dots, K$.

Consider the example in Figure 4.2 to illustrate the intuition behind the CRE algorithm. The process begins with an initial point, \mathbf{x}^0 . The critical region containing \mathbf{x}^0 , C^1 , is then computed and (4.4) is solved using the properties of C^1 . The result is the vertex \mathbf{x}^m , which is then perturbed into a neighboring unexplored critical region to \mathbf{x}^1 . Once again, the critical region containing \mathbf{x}^1 , C^2 , is computed and its properties are used to solve (4.4), resulting in \mathbf{x}^* . This is the optimal solution to this problem. However in

order to ensure that this is the case, one must explore all neighboring critical regions. So the process is repeated, where \mathbf{x}^* is perturbed to \mathbf{x}^2 , and C^4 is determined and used to solve (4.4). Now all neighboring critical regions have been explored and therefore \mathbf{x}^* is the solution. Notice, while there are four partitions in this example, only three needed to be explored in order to determine the optimal solution. If the initial point had been within C^2 or C^4 , neither C^1 nor C^3 would have needed to be explored.

4.1.1 Selecting parameter ϵ

Selection of the parameter ϵ in Algorithm 1 is the most significant difficulty in implementing CRE. From a theoretical perspective, ϵ taken to be arbitrarily small should be sufficient for convergence of the algorithm. In practice, however, ϵ is restricted by both solver precision and size of critical regions. The case of the former arises in Step 12 of Algorithm 1. This step can be formulated as a quadratic program (QP) and is frequently solved using interior-point methods which result in inexact solutions. When ϵ is set smaller than the precision of the QP solver, it is possible for the new point to lie in the same critical region as the previous point. Thus, the CRE algorithm will be unable to escape the same critical region and will cycle indefinitely without achieving the optimal point. On the other hand, the value of ϵ is upper-bounded by the size of the neighboring critical regions. If ϵ is set larger than any of the neighboring critical regions, then the next iterate may skip over a critical region and explore a non-adjacent region. The algorithm's guarantees cannot be maintained without systematic exploration of critical regions, which breaks down for large ϵ .

CHAPTER 5

NUMERICAL RESULTS

The proposed R-SCED formulation with the CRE algorithm was tested on the IEEE 14-bus and 30-bus test networks. Both cases were taken from the highly-loaded examples in PGLIB v17.08 [31]. Credible contingencies included any single line failure except those that would result in islanding in the network.

All problems were formulated in Python and suitably utilized a C++ based implementation of CRE. Linear programs and quadratic programs computed within CRE were solved by Gurobi 8.0 through its C++ interface. Simulations were performed on a 2015 Macbook Pro with a 2.7 GHz Core i5 processor and 8 GM of RAM. The subproblem constraints were augmented with slack variables to ensure feasibility.

For both test cases, the drastic action and short-term emergency limits were assumed to be 70% and 10% higher than the nominal limits, respectively. The cost associated with regulation was assumed to be equal to the nominal cost of generation.

5.1 IEEE 14-bus network results

The first example we consider is the IEEE 14-bus test network shown in Figure 5.1. The generation costs were augmented to \$20, 25, 35, 40, 45 per MWh at buses 1, 2, 3, 6, 8 respectively, and the generation capacity limits at buses 3, 6, 8 were increased from 0 to 1. The set of contingencies included all single line outages except the line between buses 7 and 8 which would result in islanding. Each contingency is assumed to occur with probability 0.005. The VoLL was set uniformly at \$90/MWh. While the VoLL is typically much higher, it is taken low for illustrative purposes.

Figure 5.2a shows that the nominal cost of generation and total load shed

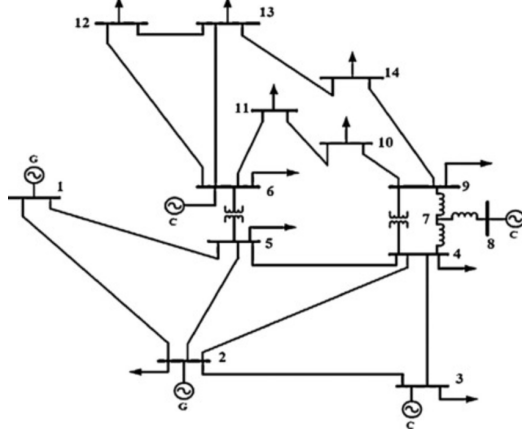


Figure 5.1: IEEE 14-bus test network.

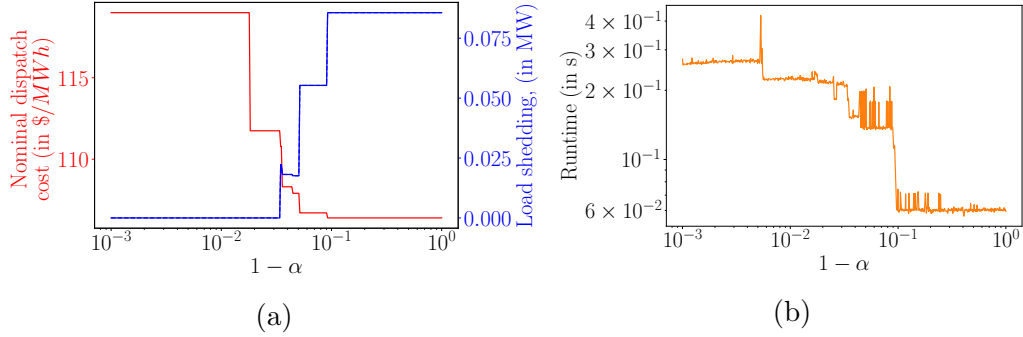


Figure 5.2: Performance of R-SCED for the IEEE 14-bus test network as a function of α , where (a) shows the effect on (—) nominal dispatch cost and (—) total load shed across contingencies and (b) shows the runtime.

are piecewise constant, as expected from Proposition 1. As the risk aversion parameter α increases to 1, the nominal cost of generation generally increases and the total load shed generally decreases. However, this behavior is not monotonic. Notice that for $\alpha \approx 0.96$, the quantity of total load shed increases as α increases. Each contingency has costs associated with load shed and regulation. In this example, the comparatively low VoLL allows for an increase in load shed for a larger decrease in regulation costs. This behavior is explored in greater detail on the IEEE 30-bus test network in Section 5.2.

5.2 IEEE 30-bus network results

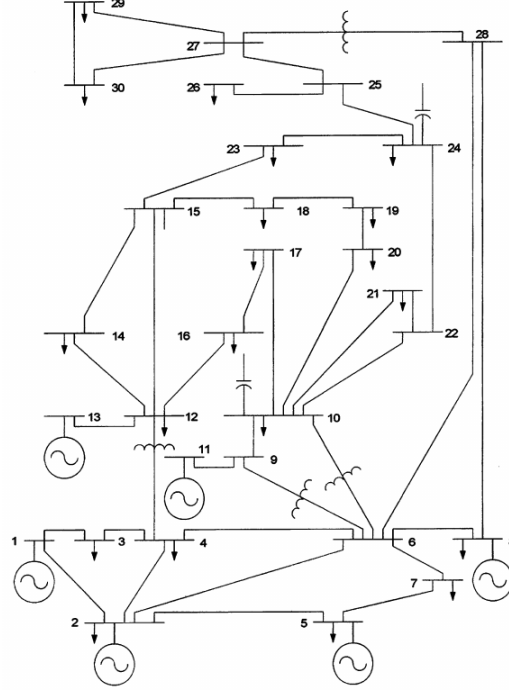


Figure 5.3: IEEE 30-bus test network.

The IEEE 14-bus network considered above had a solution that was able to meet demand without any load shed, however this is not always the case. We consider the highly-loaded IEEE 30-bus test network, shown in Figure 5.3, to understand the case when the traditional C-SCED formulation is infeasible. For this system, load shedding is imperative to ensure feasibility of the C-SCED problem. The system was augmented with generation capacity at buses 13, 22, 23, and 27 increased from 0 to 3 and cost of \$1.4, 1.8, 1.6, 1.7 per MWh, respectively. Line limits were modified as given in Table 5.1 and VoLL was assumed to be \$90/MWh at all buses. The probability of each line failing was assumed to be uniformly 0.001.

Table 5.1: Augmented line limits for IEEE 30-bus example.

Bus 1	Bus 2	Line Limit
12	16	0.33
14	15	0.396
16	17	0.36
15	18	0.319
10	20	0.312

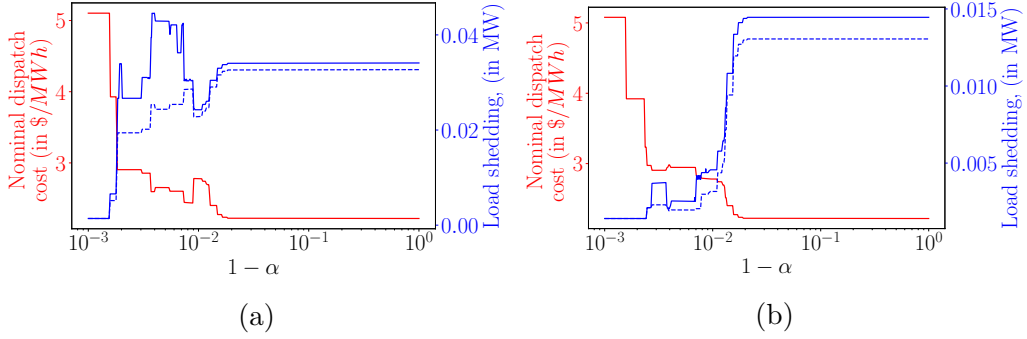


Figure 5.4: Solutions of R-SCED for IEEE 30-bus test network with uniform VoLL of (a) \$90/MWh and (b) \$126/MWh. Each figure shows (—) nominal dispatch cost, (—) total load shed, and (--) maximum load shed.

Figure 5.4 shows the results of R-SCED over the IEEE 30-bus test network. Per Proposition 1, the nominal dispatch cost and the quantity of load shed are piecewise constant. As α increases to 1, the nominal dispatch cost generally increases, however the quantity of total load shed does not generally decrease. Instead, the maximum load shed generally decreases. This behavior can be explained using the properties of CVaR. Recall that CVaR minimizes the expected tail loss and only considers cases whose cost exceeds a certain threshold. Contingencies whose cost is less than this threshold are ignored for the purpose of determining the optimal dispatch. Due to the comparatively higher cost associated with load shed, the cost threshold is defined at a point that allows for some level of load shed. Lower cost contingencies are able to shed a similar level of load if they are able to compensate by sufficiently reducing regulation to ensure the cost remains below this threshold. As a result, R-SCED allows a small quantity of load shed in contingencies with relatively low associated costs, as long as the cost of the contingency

remains below the threshold.

Similar to the IEEE 14-bus test case, the cost of nominal dispatch does not increase monotonically and the cost of load shed does not decrease monotonically with α . The objective of R-SCED balances the costs associated with load shed and regulation. This balance is captured through the VoLL. When the VoLL increases, as in Figure 5.4b, the total quantity of load shed no longer increases as dramatically with α . Instead, the load shed and nominal cost of generation are more similar to the IEEE 14-bus test case in which the load shed generally decreased and nominal cost of generation generally increased with the parameter α .

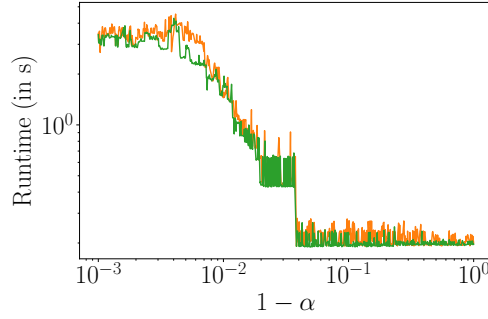


Figure 5.5: Runtime of R-SCED via CRE for VoLL of (—) \$90/MWh and (—) \$126/MWh.

The runtime of CRE for this problem is shown in Figure 5.5. For both cases, the time remains relatively constant for low α and increases with α . Intuition suggests that this increase in runtime is a product of the initial condition. As the initial condition deviates farther from the optimal solution, there are a greater number of critical regions between the initial point and the final point that CRE explores resulting in increased runtime.

CHAPTER 6

REFERENCES

- [1] O. Alsac and B. Stott, “Optimal load flow with steady-state security,” *IEEE Transactions on Power Apparatus and Systems*, no. 3, pp. 745–751, 1974.
- [2] A. Monticelli, M. Pereira, and S. Granville, “Security-constrained optimal power flow with post-contingency corrective rescheduling,” *IEEE Transactions on Power Systems*, vol. 2, no. 1, pp. 175–180, 1987.
- [3] F. Capitanescu and L. Wehenkel, “Improving the statement of the corrective security-constrained optimal power-flow problem,” *IEEE Transactions on Power Systems*, vol. 22, no. 2, pp. 887–889, 2007.
- [4] Z. Li, W. Wu, M. Shahidehpour, and B. Zhang, “Adaptive robust tie-line scheduling considering wind power uncertainty for interconnected power systems,” *IEEE Transactions on Power Systems*, vol. 31, no. 4, pp. 2701–2713, 2016.
- [5] F. Capitanescu, J. M. Ramos, P. Panciatici, D. Kirschen, A. M. Marcolini, L. Platbrood, and L. Wehenkel, “State-of-the-art, challenges, and future trends in security constrained optimal power flow,” *Electric Power Systems Research*, vol. 81, no. 8, pp. 1731–1741, 2011.
- [6] M. H. Hajiesmaili, D. Cai, and E. Mallada, “Understanding the inefficiency of security-constrained economic dispatch,” *arXiv preprint arXiv:1706.00722*, 2017.
- [7] F. Bouffard and F. D. Galiana, “Stochastic security for operations planning with significant wind power generation,” in *Power and Energy Society General Meeting-Conversion and Delivery of Electrical Energy in the 21st Century, 2008 IEEE*. IEEE, 2008, pp. 1–11.
- [8] G. Ejebe and B. Wollenberg, “Automatic contingency selection,” *IEEE Transactions on Power Apparatus and Systems*, no. 1, pp. 97–109, 1979.
- [9] S. Fliscounakis, P. Panciatici, F. Capitanescu, and L. Wehenkel, “Contingency ranking with respect to overloads in very large power systems taking into account uncertainty, preventive, and corrective actions,”

- IEEE Transactions on Power Systems*, vol. 28, no. 4, pp. 4909–4917, 2013.
- [10] D. Ernst, D. Ruiz-Vega, M. Pavella, P. M. Hirsch, and D. Sobajic, “A unified approach to transient stability contingency filtering, ranking and assessment,” *IEEE Transactions on Power Systems*, vol. 16, no. 3, pp. 435–443, 2001.
 - [11] F. Capitanescu and L. Wehenkel, “A new iterative approach to the corrective security-constrained optimal power flow problem,” *IEEE Transactions on Power Systems*, vol. 23, no. 4, pp. 1533–1541, 2008.
 - [12] F. Capitanescu, M. Glavic, D. Ernst, and L. Wehenkel, “Contingency filtering techniques for preventive security-constrained optimal power flow,” *IEEE Transactions on Power Systems*, vol. 22, no. 4, pp. 1690–1697, 2007.
 - [13] F. Bouffard, F. D. Galiana, and J. M. Arroyo, “Umbrella contingencies in security-constrained optimal power flow,” in *15th Power Systems Computation Conference, PSCC*, vol. 5, 2005.
 - [14] C. Fu and A. Bose, “Contingency ranking based on severity indices in dynamic security analysis,” *IEEE Transactions on Power Systems*, vol. 14, no. 3, pp. 980–985, 1999.
 - [15] D. T. Phan and X. A. Sun, “Minimal impact corrective actions in security-constrained optimal power flow via sparsity regularization,” *IEEE Transactions on Power Systems*, vol. 30, no. 4, pp. 1947–1956, 2015.
 - [16] T. Gomez, I. Perez-Arriaga, J. Lumbreras, and V. Parra, “A security-constrained decomposition approach to optimal reactive power planning,” *IEEE Transactions on Power Systems*, vol. 6, no. 3, pp. 1069–1076, 1991.
 - [17] J. Martínez-Crespo, J. Usaola, and J. L. Fernández, “Security-constrained optimal generation scheduling in large-scale power systems,” *IEEE Transactions on Power Systems*, vol. 21, no. 1, pp. 321–332, 2006.
 - [18] Y. Li and J. D. McCalley, “Decomposed scopf for improving efficiency,” *IEEE Transactions on Power Systems*, vol. 24, no. 1, pp. 494–495, 2009.
 - [19] D. Phan and J. Kalagnanam, “Some efficient optimization methods for solving the security-constrained optimal power flow problem,” *IEEE Transactions on Power Systems*, vol. 29, no. 2, pp. 863–872, 2014.
 - [20] Y. Liu, M. C. Ferris, and F. Zhao, “Computational study of security constrained economic dispatch with multi-stage rescheduling,” *IEEE Transactions on Power Systems*, vol. 30, no. 2, pp. 920–929, 2015.

- [21] Y. Guo, S. Bose, and L. Tong, “On robust tie-line scheduling in multi-area power systems,” *IEEE Transactions on Power Systems*, 2017.
- [22] Y. C. Chen, A. D. Domínguez-García, and P. W. Sauer, “Measurement-based estimation of linear sensitivity distribution factors and applications,” *IEEE Transactions on Power Systems*, vol. 29, no. 3, pp. 1372–1382, 2014.
- [23] P. Renaud, *Transmission Group Procedure*, http://www.nyiso.com/public/webdocs/markets_operations/services/planning/Documents_and_Resources/FERC_Form_715_Filing/Planning_Reliability_Criteria/ngrid_transmission_planning-guide.pdf, National Grid USA Service Company, Inc., 2010.
- [24] R. T. Rockafellar, S. Uryasev *et al.*, “Optimization of conditional value-at-risk,” *Journal of Risk*, vol. 2, pp. 21–42, 2000.
- [25] R. A. Jabr, “Robust self-scheduling under price uncertainty using conditional value-at-risk,” *IEEE Transactions on Power Systems*, vol. 20, no. 4, pp. 1852–1858, 2005.
- [26] Y. Zhang and G. B. Giannakis, “Robust optimal power flow with wind integration using conditional value-at-risk,” in *Smart Grid Communications (SmartGridComm), 2013 IEEE International Conference on*. IEEE, 2013, pp. 654–659.
- [27] D. Bienstock, M. Chertkov, and S. Harnett, “Chance-constrained optimal power flow: Risk-aware network control under uncertainty,” *Siam Review*, vol. 56, no. 3, pp. 461–495, 2014.
- [28] T. Summers, J. Warrington, M. Morari, and J. Lygeros, “Stochastic optimal power flow based on conditional value at risk and distributional robustness,” *International Journal of Electrical Power & Energy Systems*, vol. 72, pp. 116–125, 2015.
- [29] K. Kariuki and R. N. Allan, “Evaluation of reliability worth and value of lost load,” *IEEE Proceedings-Generation, Transmission and Distribution*, vol. 143, no. 2, pp. 171–180, 1996.
- [30] F. Borrelli, A. Bemporad, and M. Morari, *Predictive Control for Linear and Hybrid Systems*. Cambridge University Press, 2017.
- [31] “PGLib optimal power flow benchmarks,” IEEE PES Task Force on Benchmarks for Validation of Emerging Power System Algorithms, 2018. [Online]. Available: <https://github.com/power-grid-lib/pglib-opf>

APPENDIX A

DETERMINING THE CRITICAL REGION PARAMETERS

The critical region exploration algorithm presented requires determination of the affine cost structure and region over which the cost holds for each subproblem. Recall the CRE subproblem is

$$\begin{aligned} J_k^*(\mathbf{x}^0) := & \underset{\mathbf{x}^k}{\text{minimize}} && [\mathbf{c}^k]^\top \mathbf{x}^k, \\ & \text{subject to} && \mathbf{A}^k \mathbf{x}^0 + \mathbf{E}^k \mathbf{x}^k \leq \mathbf{b}^k. \end{aligned} \tag{A.1}$$

Consider fixed \mathbf{x}^0 . Assume that the minimizer $\mathbf{x}_*^k(\mathbf{x}^0)$ is unique and suppress the dependency on \mathbf{x}^0 for convenience. At the optimum, only a subset of the constraints are *active*, or bound by equality, and the rest are *inactive*. Divide the set of constraints as

$$\mathbf{A}_{\mathbb{A}}^k \mathbf{x}^0 + \mathbf{E}_{\mathbb{A}}^k \mathbf{x}_*^k = \mathbf{b}_{\mathbb{A}}^k, \tag{A.2a}$$

$$\mathbf{A}_{\mathbb{I}}^k \mathbf{x}^0 + \mathbf{E}_{\mathbb{I}}^k \mathbf{x}_*^k < \mathbf{b}_{\mathbb{I}}^k, \tag{A.2b}$$

where \mathbb{A} and \mathbb{I} denote the set of active and inactive constraints, respectively. The critical region is defined over a constant active set. Initially, assume $\mathbf{E}_{\mathbb{A}}^k$ is full rank.¹ Applying this to (A.2a),

$$\mathbf{x}_*^k = [\mathbf{E}_{\mathbb{A}}^k]^{-1} \left(\mathbf{b}_{\mathbb{A}}^k - \mathbf{A}_{\mathbb{A}}^k \mathbf{x}^0 \right), \tag{A.3}$$

over the critical region. The cost associated with the contingency is then

$$J_k^* = [\mathbf{c}^k]^\top \mathbf{x}^k = [\mathbf{c}^k]^\top [\mathbf{E}_{\mathbb{A}}^k]^{-1} \left(\mathbf{b}_{\mathbb{A}}^k - \mathbf{A}_{\mathbb{A}}^k \mathbf{x}^0 \right) = [\boldsymbol{\rho}^k]^\top \mathbf{x}^0 + \eta^k,$$

where

$$[\boldsymbol{\rho}^k]^\top := -[\mathbf{c}^k]^\top [\mathbf{E}_{\mathbb{A}}^k]^{-1} \mathbf{A}_{\mathbb{A}}^k, \quad \eta^k := [\mathbf{c}^k]^\top [\mathbf{E}_{\mathbb{A}}^k]^{-1} \mathbf{b}_{\mathbb{A}}^k.$$

¹This assumption allows for greater conceptual clarity and is often true in practice.

Recall the critical region is defined over a constant active set. Therefore, it is the region over which the inactive set remains inactive, or

$$\mathbb{P}_k := \left\{ \mathbf{x}^0 \mid \mathbf{A}_{\mathbb{I}}^k \mathbf{x}^0 + \mathbf{E}_{\mathbb{I}}^k \mathbf{x}_*^k < \mathbf{b}_{\mathbb{I}}^k \right\},$$

where \mathbf{x}_*^k is defined by (A.3). Applying this definition, the set is

$$\mathbb{P}_k := \left\{ \mathbf{x}^0 \mid \left(\mathbf{A}_{\mathbb{I}}^k - \mathbf{E}_{\mathbb{I}}^k [\mathbf{E}_{\mathbb{A}}^k]^{-1} \mathbf{A}_{\mathbb{A}}^k \right) \mathbf{x}^0 < \mathbf{b}_{\mathbb{I}}^k - \mathbf{E}_{\mathbb{I}}^k [\mathbf{E}_{\mathbb{A}}^k]^{-1} \mathbf{b}_{\mathbb{A}}^k \right\}. \quad (\text{A.4})$$

A.1 Critical region parameters under degeneracy

The previous section assumed invertibility of $\mathbf{E}_{\mathbb{A}}^k$. However, primal and dual degeneracy frequently arise when solving R-SCED. To circumvent this issue, consider the QR decomposition of $\mathbf{E}_{\mathbb{A}}^k$

$$\mathbf{E}_{\mathbb{A}}^k := \mathbf{Q} \begin{pmatrix} \mathbf{U}_1 & \mathbf{U}_2 \\ 0 & 0 \end{pmatrix}, \quad (\text{A.5})$$

where \mathbf{Q} is orthonormal and \mathbf{U}_1 is full-rank and upper triangular matrix. For convenience, let r denote the rank of $\mathbf{E}_{\mathbb{A}}^k$, and equivalently the dimension of \mathbf{U}_1 . Partition \mathbf{x} and \mathbf{c} accordingly where subscript 1 denotes the first r elements and 2 denotes the rest. Apply the transformations,

$$\mathbf{Q}^{-1} \mathbf{A}_{\mathbb{A}}^k = \begin{pmatrix} \mathbf{P}_1 \\ \mathbf{P}_2 \end{pmatrix}, \quad \mathbf{Q}^{-1} \mathbf{b}_{\mathbb{A}}^k,$$

where \mathbf{P}_1 and \mathbf{p}_1 have r rows. Suppressing the subscript $*$ in \mathbf{x}_*^k , (A.2a) can then be expressed as

$$\begin{pmatrix} \mathbf{P}_1 & \mathbf{U}_1 & \mathbf{U}_2 \\ \mathbf{P}_2 & 0 & 0 \end{pmatrix} \begin{pmatrix} \mathbf{x}^0 \\ \mathbf{x}_1^k \\ \mathbf{x}_2^k \end{pmatrix} = \begin{pmatrix} \mathbf{p}_1 \\ \mathbf{p}_2 \end{pmatrix}. \quad (\text{A.6})$$

From the first row,

$$\mathbf{x}_1^k = [\mathbf{U}_1]^{-1} (\mathbf{p}_1 - \mathbf{P}_1 \mathbf{x}^0 - \mathbf{U}_2 \mathbf{x}_2^k).$$

The cost associated with these first r variables is then

$$[\mathbf{c}_1^k]^\top \mathbf{x}_1^k = [\mathbf{c}_1^k]^\top [\mathbf{U}_1]^{-1} (\mathbf{p}_1 - \mathbf{P}_1 \mathbf{x}^0 - \mathbf{U}_2 \mathbf{x}_2^k).$$

Consider the partition of the inactive set, (A.2b), corresponding to our partition of \mathbf{x}_*^k

$$\mathbf{A}_{\mathbb{I}}^k + \begin{pmatrix} \mathbf{F}_1 & \mathbf{F}_2 \end{pmatrix} \begin{pmatrix} \mathbf{x}_1 \\ \mathbf{x}_2 \end{pmatrix} < \mathbf{b}_{\mathbb{I}}^k.$$

The critical region is the intersection of set where the inactive constraints remain inactive and \mathbf{x}^0 satisfies the constraint arising in the second row of (A.6),

$$\mathbb{P}_k := \left\{ \mathbf{x}^0 \left| \exists \mathbf{x}_2 \text{ such that } \mathbf{P}_2 \mathbf{x} = \mathbf{p}_2, \begin{pmatrix} \mathbf{x}^0 \\ \mathbf{x}_2 \end{pmatrix} \in \mathbb{C}_k \right. \right\},$$

where

$$\mathbb{C}_k := \left\{ \begin{pmatrix} \mathbf{x}^0 \\ \mathbf{x}_2 \end{pmatrix} \left| \left(\mathbf{A}_{\mathbb{I}}^k - \mathbf{F}_1 [\mathbf{U}_1]^{-1} \mathbf{P}_1 \right) \mathbf{x}^0 + \left(\mathbf{F}_2 - \mathbf{F}_1 [\mathbf{U}_1]^{-1} \mathbf{U}_2 \right) \mathbf{x}_2 < \mathbf{b}_{\mathbb{I}}^k - \mathbf{F}_1 [\mathbf{U}_1]^{-1} \mathbf{p}_1 \right. \right\}.$$